Fuel 424 (2026) 139339

Contents lists available at ScienceDirect

Fuel

journal homepage: www.elsevier.com/locate/fuel

Full Length Article

Kinetic study and confirmation of epoxide-dependent oligomerization of methyl oleate

Julian Türck [a,b,*], Carsten Funke [c], Fabian Schmitt [b], Jan Schneider [c], Hans-Jürgen Danneel [c], Ralf Türck [b,d], Wolfgang Ruck [a], Jürgen Krahl [d,e]

[a] School of Sustainability, Leuphana University Lüneburg, Universitätsallee 1, C11.012, 21335 Lüneburg, Germany
[b] Tecosol GmbH, Jahnstraße 2, 97199 Ochsenfurt, Germany
[c] OWL University of Applied Sciences and Arts, Institute for Life Science Technologies ILT.NRW, Department of Life Science Technologies, Campusallee 15, 32657 Lemgo, Germany
[d] Fuels Joint Research Group, Germany
[e] OWL University of Applied Sciences and Arts, Campusallee 12, 32657 Lemgo, Germany

ARTICLE INFO

Keywords:
Biodiesel aging
Epoxide-dependent oligomerization
Acetic acid
Identification of aging products
Kinetics of aging products

ABSTRACT

The aging of biodiesel proceeds via multiple pathways, with oligomerization playing a central role. In this study, we investigated an epoxide-dependent oligomerization pathway, which had previously only been postulated. Using methyl oleate (C18:1) as a model monounsaturated fatty acid and acetic acid as a representative, reactive nucleophile and known biodiesel aging product with a suitable boiling point, oligomeric products were identified by size-exclusion chromatography (SEC) coupled with electrospray ionization quadrupole time-of-flight mass spectrometry (ESI-QTOF-MS). The concentration of 20 wt% was chosen to ensure a measurable kinetic effect while maintaining stable reaction conditions. Furthermore, the role of methyl oleate during biodiesel aging was addressed. Time-resolved analysis confirmed the proposed sequential order of reactions. It was pointed out that elimination reactions may occur. The data support the formation of epoxides, despite the isobaric overlap with ketones, and show that hydroxyl intermediates undergo esterification and etherification. Moreover, experiments with pure C18:1 demonstrated that acetic acid–derived oligomers are generated. Under Rancimat conditions, addition of 20 wt% acetic acid resulted in an approximately 1.1 – 2.6 increase in product yield. Kinetic analysis revealed structure-dependent formation and decay behavior of the aging products, with slightly faster epoxidation and shifted product distributions toward higher oligomeric species in the presence of acetic acid. Reactive intermediates were consumed more rapidly than oligomeric species and all decay processes followed apparent second-order kinetics. These findings provide direct experimental evidence for the involvement of epoxide-dependent pathways in biodiesel aging.

1. Introduction

The substitution of fossil fuels and the emergence of new renewable fuels lead to complex interactions between the components. In order to develop an ideal fuel, it is essential to understand the influence of each individual component on the fuel properties. An important parameter is fuel aging. This describes the change of chemical and physical properties in the fuel over a defined period of time Tuerck et al. [1]. Due to the rising popularity of hybrid vehicles, this parameter becomes increasingly important. In the complex mechanism of fuel aging, the oxidation of fuels is the first crucial step. Biodiesel (FAME) is an example of a market-established fuel that is susceptible to oxidation. The properties of FAME itself are determined by the fatty acid composition of the raw material Ramos et al. [2], Miraboutalebi et al. [3]. The cold resistance of FAME is determined by the degree of unsaturation of its fatty acids Kleinová et al. [4]and the carbon chain length Yuan et al. [5]. However, the double bonds serve as primary sites for oxygen attack. Reactivity rises with the number of double bonds (mono < allylic < bis-allylic) Wang, C.-c., et al., et al. [6]. The C18 fatty acid series is a convenient example of this reactivity series, since linoleic acid (C18:2) and linolenic acid (C18:3) oxidize more rapidly due to lower C–H dissociation energies with increasing unsaturation [7]. In general, the initial oxidation

* Corresponding author.
E-mail address: julian.tuerck@stud.leuphana.de (J. Türck).

https://doi.org/10.1016/j.fuel.2026.139339
Received 22 October 2025; Received in revised form 13 February 2026; Accepted 28 March 2026
Available online 3 April 2026
0016-2361/© 2026 The Author(s). Published by Elsevier Ltd. This is an open access article under the CC BY license (http://creativecommons.org/licenses/by/4.0/).

of FAME is described by autoxidation Longanesi et al. [8]. Analogous to lipid peroxidation, peroxides are formed first [9], which are initiators for radical decomposition Zuleta et al. [10]. This radical process leads to various oxidative decomposition products. An indicator of this is the acid value, as new carboxyl functionalities are formed [11]. Examples include short-chain carboxylic acids such as formic acid and acetic acid [12]. In general, the kinetics of the formation of different aging product groups play an essential role in understanding the sequential order of an aging scheme. An example of this is the study by Türck et al., who used oxidation kinetics to identify the reaction chain peroxide->acid->epoxide->ketone Türck et al. [13]. At a certain point, FAME aging transitions into oligomerization Fang [14]. Different reaction pathways can occur here. The occurrence of these oligomers in engine oil is particularly noticeable because FAME can dilute the engine oil due to late in-cylinder approach and low temperature distillation of methyl esters Singh et al. [15].

One possibility how oligomers can be formed was postulated by Türck et al. Türck et al. [13]. Here, it is described that the oxidative decomposition products can interact and react with unaltered FAME due to the reactivity of various functional groups. A correlation between the acid value of the FAME and the epoxide content was observed, which indicated an in situ Prileschajew reaction Türck et al. [13]. It has been described that aldehydes can form peroxy acids in situ under thermo-oxidative conditions. The Prileschajew reaction is shown in Fig. 1.

Furthermore, these epoxides demonstrated that they could undergo epoxide opening reactions with nucleophiles (see Fig. 2). Using ESI-QTOF-MS, it was measured that, for example, isopropylidene glycerine (solketal) can attack an electrophilic carbon with its hydroxyl group. The same was observed with both 1-octanol and octanoic acid. Size exclusion chromatography (SEC) provided an overview of the formation of dimers, trimers and even tetramers. In general, the publication used a nomenclature which simplifies dimers as an aging product formed by an addition reaction. The same applies to further reactions (trimers, tetramers, etc.). It was observed that the addition of octanoic acid, solketal, etc. led to fewer trimers and tetramers but more dimers. This suggested that the epoxide opening reaction could have an influence on oligomerization. An oligomerization diagram was derived from this, which is shown in Fig. 3. This diagram was developed on the basis of plausibility and literature. Depending on the nucleophile interacting with epoxide, progressive reactions are imaginable. If the nucleophile has one functional group, a ‘quenching’ of the oligomerization process is conceivable. If a second or more functional groups occur, these can then react with other aging products. It is also feasible that the hydroxyl group formed during epoxide opening takes different reaction pathways. The formation of ethers and esters, oxidation to a ketone and elimination by acids and water are possible. Analogous to the first step, the double bonds could form epoxides again, followed by epoxide opening reactions. Previous studies have generally shown that epoxides in cottonseed oil and the respective fatty acid methyl esters contribute to oligomerization processesMeng et al. [16].

The aim of this work was to confirm the formation of oligomers in the oligomerization scheme under rancematic conditions by MS measurements. In addition, the role of methyl oleate in the aging of biodiesel should be demonstrated. Acetic acid was selected because it is a well-documented biodiesel aging product and a small, highly mobile carboxylic acid that can act as an efficient nucleophile, thereby directly probing acid-/nucleophile-promoted epoxide ring-opening and subsequent esterification pathways. A concentration of 20 wt% was employed to provide a sufficiently high nucleophile activity to yield measurable, statistically robust changes in formation and decay kinetics while maintaining a single-phase, experimentally manageable reaction mixture compatible with the aging setup and analytical workflow. C18:1 was selected as a model compound because it represents a structurally well-defined monounsaturated fatty acid ester containing a single isolated double bond, thereby providing a simpler and more controlled system than allylic or bis-allylic polyunsaturated analogues. In comparison to these more reactive systems, its reduced susceptibility to oxidation and radical side reactions enabled clearer kinetic evaluation and more unambiguous identification of intermediates and product. Furthermore, the kinetics of the formation of the aging products were investigated to obtain an overview of the postulated course of the scheme.

2. Results and discussion

2.1. Identification of the oligomers

First, a qualitative assessment was made to determine whether the aging products were formed in accordance with the oligomerization scheme. Table 1 lists the aging products which were generated in the presence of acetic acid. It also shows which oligomers were qualitatively sought, identified and confirmed. The following section shows reaction mechanisms that are part of the oligomerization mechanism based on the measurement of the molecular mass of aging products. Acetic acid was chosen since it exhibited high nucleophilic reactivity with low steric hindrance. Furthermore, its boiling point exceeded the reaction temperature, making it preferable to e.g. formic acid.

The division into dimers and trimers corresponds to the publication by Türck et al. Türck et al. [13]. For simplicity, each aging product had been given a name according to its functional group (see Table 1). Since the methyl ester group of C18:1 was not taken into account, this functional group was not included in the nomenclature. Furthermore, SEC-MS did not allow the exact determination of the positions at which the functional groups are bound in the carbon chain. Due to the relatively low concentrations and the polydisperse and complex nature of the system in terms of purification, the individual aging products were not isolated. In addition, the complex purification process would have had an impact on the determination of kinetics.

Starting from epoxide, the hydroxy-ester formed by the epoxide opening was the starting molecule for progressive oligomerization. In the next step, the oxidation of the hydroxyl group to ketone occurred under the thermo-oxidative conditions of Rancimat-derived aging. In general, the formation of ketones is not novel since ketones can be generated during radical degradation of peroxides Flitsch et al. [17]. However, the ESI-QTOF-MS measurement indicated that the direct oxidation of the secondary hydroxyl group to the respective ketone during fuel aging took place. Due to the absence of further reactive groups, the ketone-ester should be more stable compared to other oligomers. However, the electrophilic carbon of the ketone is a reactive site for nucleophiles. Under these reaction conditions, no such reaction was observed. The verified di-ester also showed that the hydroxyl group of the hydroxy-ester can react directly with acetic acid (see Fig. 4).

Another possibility was to eliminate the hydroxyl group to create a double bond. This was feasible due to the presence of water[18]and the

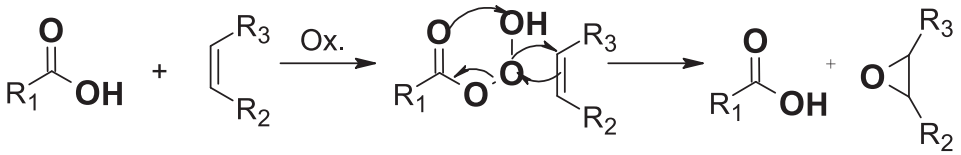

Fig. 1. Reaction mechanism of Prileschajew Reaction. Carboxylic groups build up peroxy acids to epoxidize double bonds.

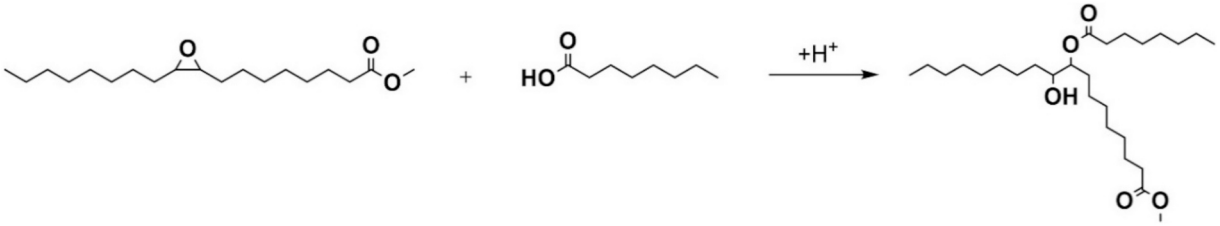

Fig. 2. Acid-catalyzed epoxide opening reaction with a nucleophile. This example describes the reaction of 9,10-epoxy stearate with octanoic acid.

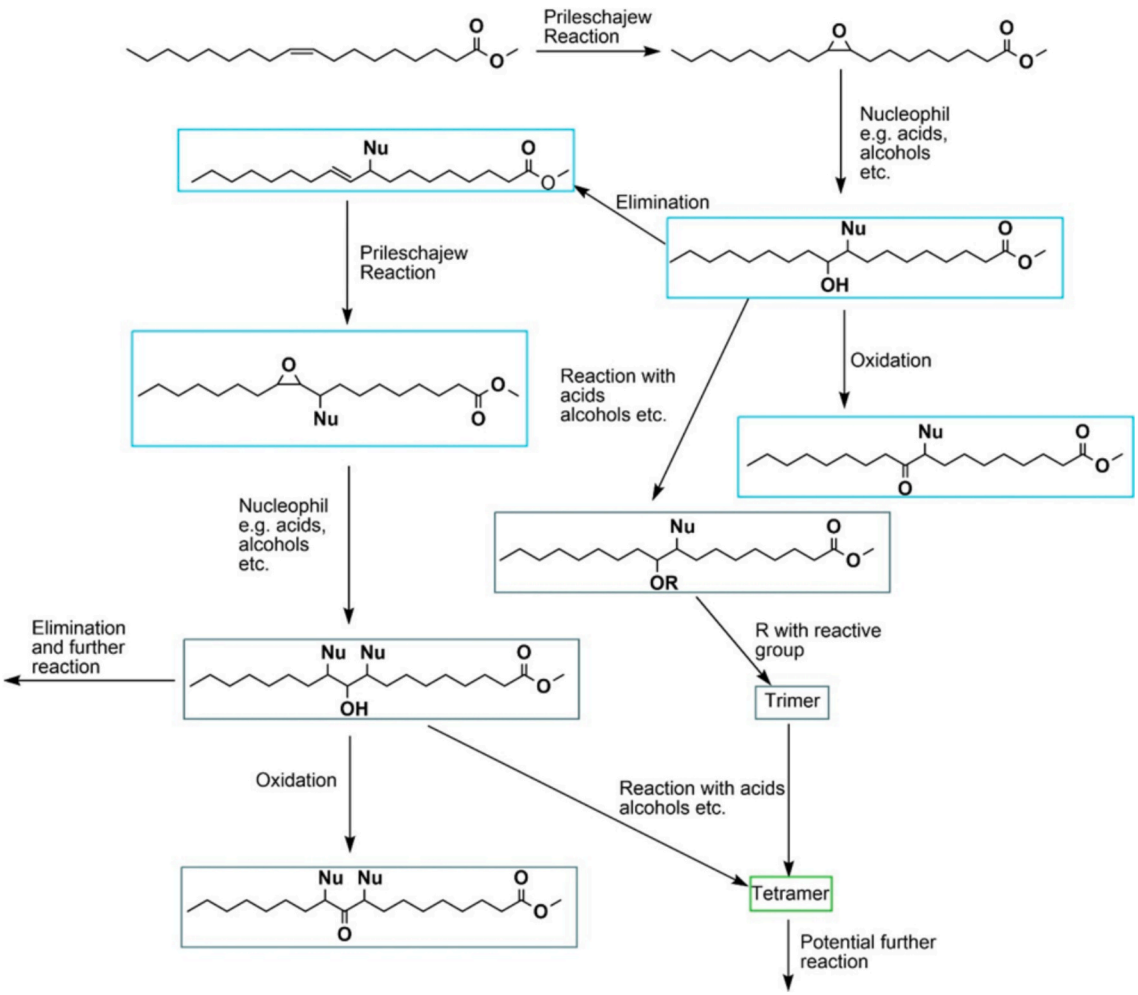

Fig. 3. Epoxide dependent oligomerization scheme taken from (Türck, Schmitt et al. 2023). The colors depict the class of oligomer. Turquoise: Dimer, grey: Trimer and green: Tetramer. (For interpretation of the references to colour in this figure legend, the reader is referred to the web version of this article.)

increase in acid value during biodiesel agingTürck et al. [19]. Using ESI-QTOF-MS, the molecular mass of the alkene was measured with high mass accuracy (<2 mDa), providing strong evidence for an elimination reaction. Furthermore, the mass of the sp^3-hybridised molecule fell outside the error range in both positive and negative MS modes. Fig. 5 shows the elimination reaction of the hydroxy-ester to create the alkene-ester.

It shows the general mechanistic process via oxonium ion formation, since the hydroxyl group did not constitute a good leaving group. Due to the oxonium ion, it was probable that the mechanism proceeds via E_1 elimination, which would create carbocation. However, since the exact position of the hydroxyl group had not been determined, it was unclear where the carbocation was formed. As a result, the position of the double bond could not be determined. Alkenes, like unsaturated fatty acids, are susceptible to oxidation under rancematic conditions. This leads to the formation of peroxides, hydroxyl groups, ketones, etc. Yaakob et al. [20]. However, the oligomerization scheme depicted acid dependent epoxidation. This double bond can thus be epoxidized again, similar to the first epoxidation, to form the epoxy-ester. One challenge was to distinguish between epoxy-ester and ketone-ester, as both molecules are isobars. In general, epoxides and ketones can be differentiated by fragmentation. Epoxides yield characteristic 16 *m/z*Feng et al. [21]and formaldehyde 29 *m/z* fragmentsKoritzke et al. [22]. Like other carbonyl compounds, ketones exhibit the characteristic fragment 28 *m/z* (loss of C=O), which is the result of McLafferty rearrangements Sparkman et al. [23]. Regardless of its epoxide function, however, the epoxy-ester possesses two carbonyl groups (acetate and methyl ester). Furthermore, the low concentration and complexity of the samples due to similar retention times made it difficult to detect the 16 *m/z* fragment. However, since the alkene-ester had been detected and epoxidation occurred

Table 1
List of investigated oligomers induced by acetic acid. A distinction is made between dimers and trimers. The starting point for the analysis is the epoxide. In addition, a study-specific nomenclature is introduced for further discussion.

Molecule class	Chemical structure	Name	Molecular weight [Da]	Averaged measured mass error [mDa]
Origin	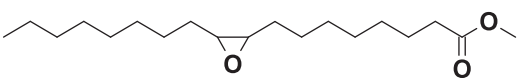	Epoxide	312.494	1.6
Dimer	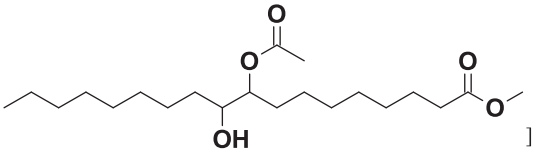	Hydroxy-ester	372.546	1.6
Dimer	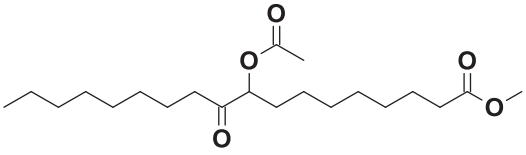	Ketone-ester (Isobar of epoxy-ester]	370.530	0.8
Dimer	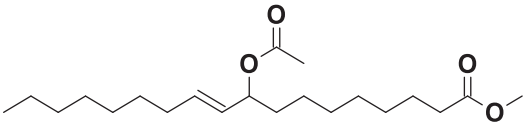	Alkene-ester	354.531	0.3
Dimer	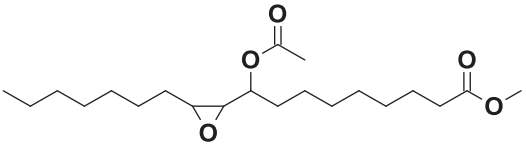	Epoxy-ester (Isobar of ketone-ester]	370.530	0.8
Trimer	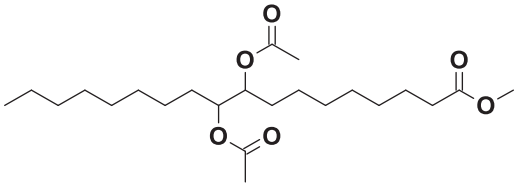	Di-ester	414.583	1.7
Trimer	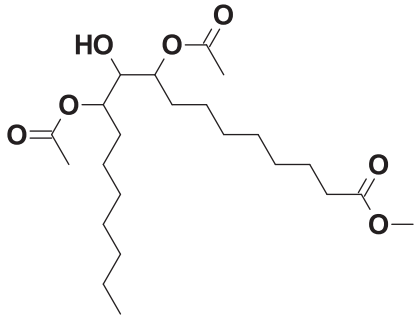	Hydroxy-di-ester	430.582	1.5

(*continued on next page*)

Table 1 (*continued*)

Molecule class	Chemical structure	Name	Molecular weight [Da]	Averaged measured mass error [mDa]
Trimer	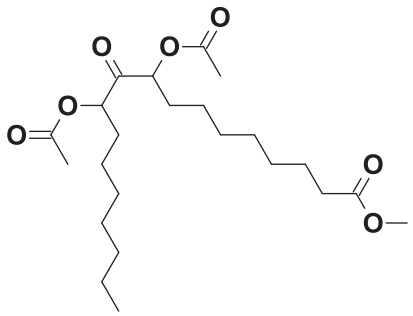	Ketone-di-ester	428.566	0.5

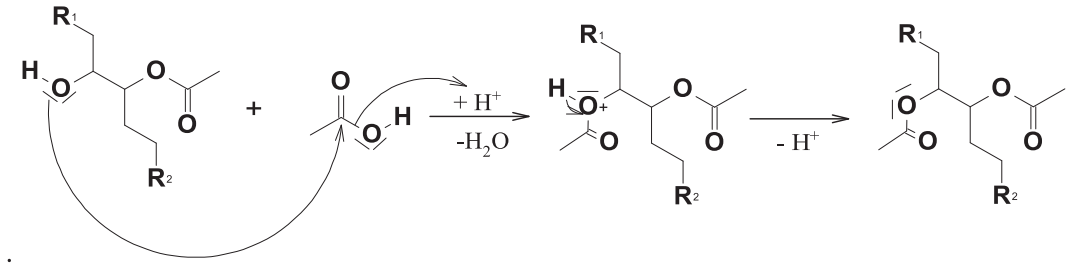

Fig. 4. Acid-catalyzed esterification of hydroxy-ester with acetic acid to give the di-ester.

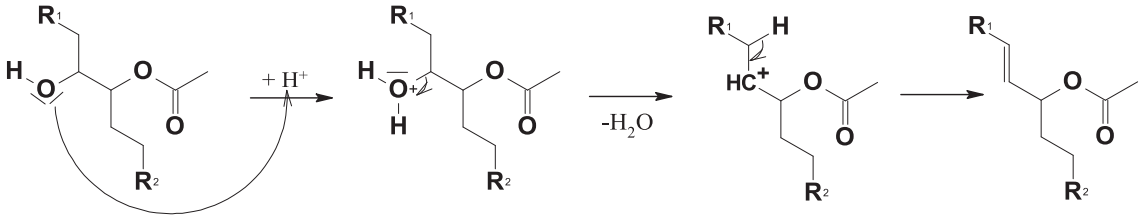

Fig. 5. General reaction mechanism: acid-catalyzed elimination reaction via oxonium ions to generate an alkene functionality.

during aging, epoxides should also be produced. The plausibility assessment was supported by the fact that the trimers, both hydroxy- and

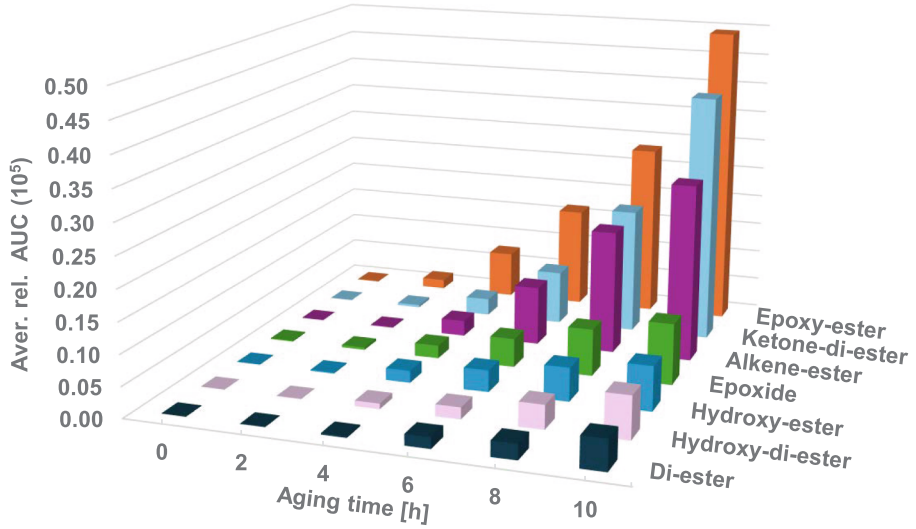

Fig. 6. 3D plot of the first 10 h of the aging of C18:1 with 20 wt% acetic acid (in 2-hour increments). Depicted are the averaged relative areas under the curve (AUC) for each Rancimat-derived aging product (Di-ester: dark blue, hydroxy-di-ester: light red, hydroxy-ester: marine, epoxide: green, alkene-ester: purple, ketone-di-ester: light blue, epoxy-ester: orange) (n = 3). (For interpretation of the references to colour in this figure legend, the reader is referred to the web version of this article.)

ketone-di esters, were measured. These molecules should mainly be derived from a second epoxide opening reaction of the epoxide-ester.

Further follow-up reactions of the trimers were conceivable, but increasingly unlikely due to the low concentration. The hydroxy-di-ester can react further due to the reactivity of the hydroxyl group. However, these reactions are also sterically hindered due to the number of acetate groups on C18:1. It is also feasible that some of the methyl esters undergo acid hydrolysis which could lower the yield.

2.2. Time-resolved formation and decay of epoxide-dependent products

After the oligomers of the epoxide dependent oligomerization had been identified, the next step was to confirm the sequence of the molecule formation. For this purpose, the aging products were quantified over a defined aging time. It showed the sequence in which the oligomers were formed and when they decompose. In order to obtain a reference for the natural aging of C18:1, the time course was also carried out with pure C18:1. Figs. 6 and 7 display the development of aging products over a period of 10 h in 2-hour increments for the blends with and without acetic acid.

The plots for the individual aging products are shown in supporting information. The error bars (std. dev.) are displayed there and demonstrate how reproducible the measurements are. These findings serve to support the argumentation regarding the sequence of aging products. In general, it became evident that blending acetic acid resulted in the formation of more acetic acid-based aging products. However, taking into account the weight proportion of the added acetic acid, the difference in product formation during the first 10 h was not significantly greater. One reason for this observation can be found in the experimental setup. Since there was no cooling device, some of the acetic acid evaporated. However, Table 2 shows that with the Rancimat setup, a higher yield was achieved. For comparison, the value at 10 h is used.

The greatest increases occurred for the trimers, while the di-ester showed the most significant increase (factor 2.65) due to blending with acetic acid. The hydroxy-ester was the only aging product to show a decrease (factor 0.87). However, the other sequential aging products based on the hydroxy-ester experienced an increase in yield due to acetic acid blending. This could be an indication of a change in kinetics. With regard to the formation of aging products over time, both blend systems showed comparable behavior. Within the first two hours, hardly any products were detectable, while the ketone/epoxide-ester peak was already forming. After four hours, significant amounts were present, which continued to increase until the tenth hour. It was noticeable that the epoxide did not achieve the highest signal intensity despite its role as the starting point of the scheme. Due to the correlation between acid number and epoxide value described in Türck et al. [19], a higher epoxide value would have been expected. However, the relatively small errors in the AUC values indicate that its role as the starting product is plausible (see supporting information). One possible reason for the comparatively low concentration is the high reactivity of the epoxide. A similar explanation also applies to the hydroxy-ester, which is reactive and particularly susceptible to oxidation. The oxidation of the hydroxyl group became evident for the trimers, as well. For those significantly more ketone-di-esters than hydroxy-di-esters were formed (factor 5.9–6.1 for both blend systems). In addition, the formation of alkene-esters was more prominent than that of epoxide-esters. This supports the hypothesis that the alkene-ester acts as a precursor and can undergo epoxidation reactions. Overall, it became clear that comparatively small amounts of di-esters were formed in the first 10 h.

Since the first 10 h represented the onset of aging, a more comprehensive view of time course was required. For this purpose, the blends were aged at 10-hour increments for 100 h (Fig. 8). The respective 3D plot without acetic acid is illustrated in the supporting information. This screening helped to confirm that the molecules had been properly classified as dimers or trimers. All dimers reached their peak at 20 h, whereas trimers tended to peak at around 40 to 50 h. Only the peak of the di-ester behaves differently, as it is a trimer but is located at 20 h. However, the earlier peak does not represent a contradiction, as the direct reaction of the hydroxyl group with the acetic acid should proceed faster than the formation of the other trimers. In terms of peak time, this is more comparable to elimination, which was observed. In addition, the

Table 2
Calculated factors for aging products. The factor displays the ratio between C18:1 + acetic acid and pure C18:1.

Aging product	Factor
Epoxide	1.23
Hydroxy-ester	0,87
Alkene-ester	1.21
Ketone/epoxy-ester	1.13
Di-ester	2.65
Hydroxy-di-ester	1.3
Ketone-di-ester	1.26

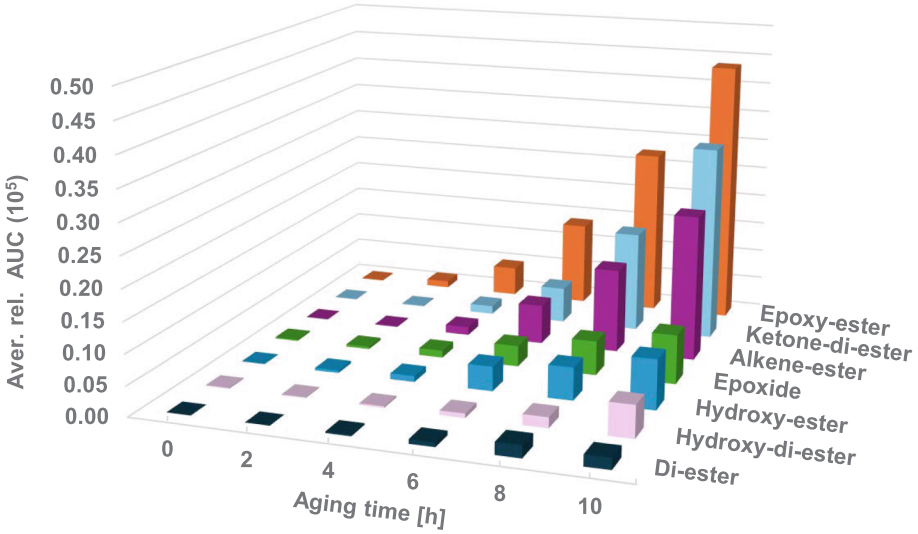

Fig. 7. 3D plot of the first 10 h of the aging of pure C18:1 (in 2-hour increments). Depicted are the averaged relative areas under the curve (AUC) for each Rancimat-derived aging product (Di-ester: dark blue, hydroxy-di-ester: light red, hydroxy-ester: marine, epoxide: green, alkene-ester: purple, ketone-di-ester: light blue, epoxy-ester: orange) (n = 3). (For interpretation of the references to colour in this figure legend, the reader is referred to the web version of this article.)

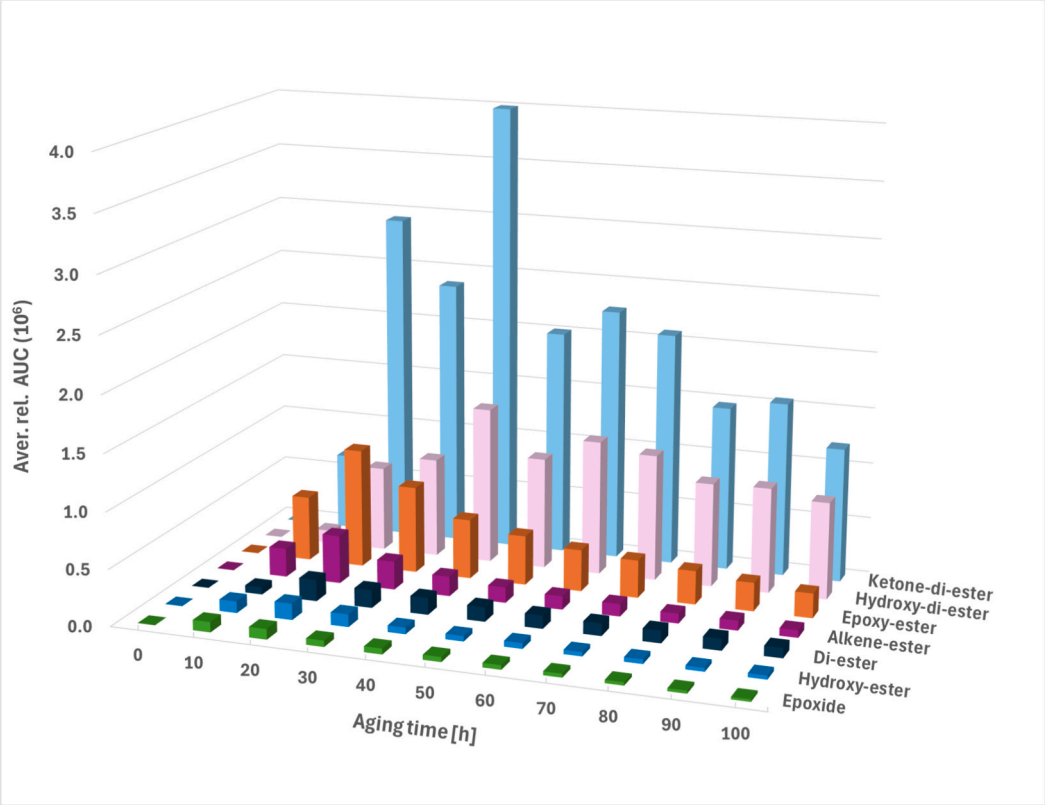

Fig. 8. 3D plot of the 10 to 100 h of the aging of C18:1 with 20 wt% acetic acid (in 10-hour increments). Depicted are the averaged relative areas under the curve (AUC) for each Rancimat-derived aging product (Di-ester: dark blue, hydroxy-di-ester: light red, hydroxy-ester: marine, epoxide: green, alkene-ester: purple, ketone-di-ester: light blue, epoxy-ester: orange) (n = 3). For clarity, the order of the data series in the 3D plot was adjusted, with the most intense bars placed at the back and the least intense at the front, to avoid overlapping and ensure visibility of all data. The color scheme assigned to each series was preserved. (For interpretation of the references to colour in this figure legend, the reader is referred to the web version of this article.)

error increased from dimer to trimer, which was a result of competitive reactions (see supporting information). Furthermore, the increase in errors, as in the first 10 h, was an indication of the proposed sequence. This corresponds with Türck et al., who showed that a change in kinetics occurs at this particular aging time Türck et al. [19]. As the reaction progressed, it became evident that both the ketone- and the hydroxy-di-ester were formed in the highest quantities. In general, more ketone-di-ester was generated than hydroxy-di-ester (factor 1.39 for 100 h with acetic acid). At the highest value at 40 h, they differ by a factor of 2.86. The decrease in Ketone-di-ester from 50 to 100 h indicated that it undergoes follow-up and/or decomposition reactions and is not a stable end product. Furthermore, it had been demonstrated that significantly fewer epoxides and dimers, which acted as intermediate products, were formed.

The time-resolved analysis is a further supportive investigation that supports the aging sequence that was postulated. The alkene-ester, which accounted for a larger proportion in the first 10 h (see Figs. 6 and 7), tended to show lower intensity than the ketone- and epoxy-esters. The earlier degradation suggested that the proposed trimers are subsequent products. To assess the influence of acetic acid on the kinetics of the aging products, the corresponding build-up and decay rate constants were determined.

2.3. Kinetics of the epoxide-depending products

In order to obtain an initial estimate of the formation kinetics, the first 10 h of the experiments shown in Figs. 6 and 7 were analyzed to determine the apparent build-up rate constants. As already shown in Table 2, blending with acetic acid resulted in an increased formation of aging products. Table 3 compares pure C18:1 with C18:1 containing 20 wt% acetic acid.

Table 3
Build-up rate constants of the aging products for pure C18:1 and C18:1 + acetic acid. The reported factor corresponds to the ratio of the rate constant with acetic acid to that of the pure system.

	Build-up rate constant [h^{-1}]		
Aging product	Pure C18:1	C18:1 + acetic acid	Factor
Epoxide	0.36	0.44	1.22
Hydroxy-ester	0.54	0.51	0.94
Alkene-ester	0.94	0.97	1.03
Ketone/epoxy-ester	0.59	0.60	1.02
Di-ester	0.88	0.50	0.57
Hydroxy-di-ester	0.34	0.55	1.62
Ketone-di-ester	0.67	0.95	1.42

Considering the observed influence on the Prileschajev reaction, the formation kinetics indicated that epoxidation proceeded approximately 1.22-fold faster in the presence of acetic acid. For intermediate species, including the hydroxy-ester, alkene-ester, and ketone/epoxy-ester, no clear differences in the formation rate constants were detected between systems with and without acetic acid. In these cases, both the build-up kinetics and the subsequent conversion may already have approached a quasi-steady state, thereby masking potential rate differences. The accelerating effect of acetic acid was further supported by the faster formation of the ketone-di-ester and hydroxy-di-ester. As both species represent trimeric products and therefore correspond to more advanced stages of the reaction sequence, their formation rates were likewise increased in the presence of acetic acid, accompanied by higher overall concentrations of aging products. In contrast, the formation of the di-ester was reduced under these conditions. This behavior may indicate

that acetic acid, due to its pK_a, facilitated elimination of the hydroxyl group and thereby altered the preferred reaction pathway. To further quantify these observations, the decay kinetics were subsequently evaluated. Evaluation of the decay kinetics using different reaction orders showed that, for all species, the coefficient of determination (R^2) was most consistent with second-order behavior (see supporting information). The corresponding rate constants are summarized in Table 4.

Overall, the observed kinetics revealed distinct classes of decay rate constants that appeared to reflect systematic differences in molecular structure and reactivity. In agreement with the proposed reaction schemes, the decay rate constant progressively decreased from the monomeric epoxide to the dimeric and trimeric species, suggesting that increasing oligomer size reduced functional group accessibility and reactivity, potentially due to steric and diffusional limitations. The comparatively high decay rate constant of the hydroxy-ester supports its proposed role as a reactive branching intermediate from which multiple competing reaction pathways may have originated, thereby accelerating its overall consumption. In contrast, the alkene-ester exhibited the largest decay rate constant, plausibly reflecting the enhanced reactivity of the carbon–carbon double bond. The epoxy-ester and di-ester degraded on similar timescales, indicating comparable intrinsic stabilities. Notably, the later-formed hydroxy-di-ester and keto-di-ester species displayed the slowest decay, in line with the oligomerization scheme and suggesting that these compounds represented comparatively stable products within the reaction network. In comparison, the acetic acid blends showed decay rate constants of a similar order of magnitude compared to pure C18:1 for all aging products. However, with the exception of the hydroxy-di-ester, these blends generally exhibited lower rate constants than pure C18:1. Similar to the trends observed during the build-up phase, these results suggest that acetic acid may promote alternative reaction pathways that compete with oxidation.

3. Conclusion and outlook

In general, this study supports the postulation of epoxide-dependent oligomerization. The masses of the oligomers resulting from acetic acid were measured using SEC coupled to ESI-QTOF-MS. However, looking at pure C18:1 shows that artificial blending doesn't cause unusual C18:1 aging products. It turns out that these aging products can occur under Rancimat-induced conditions.

Based on the plausibility and successful identification of the Prileschajew analogue and the epoxide opening reaction, various reaction pathways for the resulting hydroxyl group were proposed. Further epoxidation was indicated by measuring the alkene-ester and the resulting hydroxy- and ketone-di-ester products formed from the respective epoxide. Furthermore, observations of alkene-esters suggest that elimination reactions may occur during the aging of biodiesel. The same applies to the di-ester, which demonstrates that hydroxyl groups generated during aging can undergo esterification or etherification reactions. In addition, time-resolved analysis supports the sequential order of aging products. It appears that the peak of the trimers occurs later than that of the dimers. Degradation begins after 40 h, which confirms this point in time is special for the aging of C18:1. In general, the addition of acetic acid causes two times more aging products to be formed in the first 10 h, except for hydroxy-ester (factor 1.18). The kinetic analysis revealed that acetic acid modestly accelerated epoxidation while selectively influencing downstream aging pathways and promoting the formation of higher oligomeric species. Decay analysis indicated structure-dependent stability, as reactive intermediates were consumed more rapidly whereas larger oligomeric species persisted longer, and all species followed apparent second-order kinetics. Collectively, these findings suggest that acetic acid mainly affected the relative contribution of competing pathways, while leaving the intrinsic kinetics of the system largely unchanged.

After a further step has been taken to confirm the epoxide-dependent oligomerization scheme, the next stage involves investigating the impact of aging under reflux. It is feasible that a higher concentration of aging products will be obtained. This may facilitate the analysis of subsequent products. In addition, the individual aging products could be isolated. With the help of chromatographic separation followed by scheduled isolation and fragmentation of the molecules within the quadrupole and the collision cell of the MS device, MS/MS spectra could be acquired in order to distinguish between the ketone- and epoxy-ester. Furthermore, the positions of the functional group in the carbon chain should be determined. Apart from that, the investigation should be examined with other nucleophiles. On the one hand, to evaluate the steric effect with, for example, formic acid and propionic acid, on the other hand, to investigate the reactivity (e.g. hydroxyl vs. carboxylic group). Further studies isolating other fatty acids could also identify additional reaction pathways and define the roles of individual components and functions more precisely.

Table 4
Decay rate constants of the aging products for pure C18:1 and C18:1 + acetic acid. The reported factor corresponds to the ratio of the rate constant with acetic acid to that of the pure system.

		Decay rate constant [µLcounts^{-1}h^{-1}]	
Aging product	Pure C18:1	C18:1 + acetic acid	Factor
Epoxide	4.87E-06	4.18E-06	0.86
Hydroxy-ester	3.69E-06	2.84E-06	0.77
Alkene-ester	1.89E-06	1.44E-06	0.76
Ketone/epoxy-ester	5.66E-07	4.32E-07	0.76
Di-ester	8.32E-07	6.73E-07	0.81
Hydroxy-di-ester	3.89E-08	6.05E-08	1.56
Ketone-di-ester	9.00E-08	8.14E-08	0.91

4. Experimental section

4.1. Chemicals and reagents

C18:1-methyl ester (methyl oleate, purity 99 %) and glacial acetic acid (analytical grade) were purchased from Merck KGaA, Germany. C18:1 was mixed with 20 % (v/v) glacial acetic acid to induce chemical modification. Ethanol (LC-MS grade), formic acid (≥99 %, LC-MS grade), and ultra-pure water were obtained from AppliChem GmbH, Germany. All solvents were filtered through 0.20 µm PES membranes from Altmann Analytik GmbH & Co. KG, Germany, prior to use.

4.2. Fuel aging and sample preparation

Fuel aging was carried out using a Metrohm 743 Rancimat device. The measurement was done according to EN 14112. The sample was heated under a constant stream of air, which accelerated oxidation and evaporated volatile secondary oxidation products such as short chain carboxylic acids into a measuring vessel containing water (eluate). Homogeneous mixing of the reaction solution was ensured by the continuous airflow. The increase in water conductivity, caused by dissolved low-molecular acidic compounds, was continuously monitored and used to determine the oxidation induction time. Each measurement was repeated three times to assess reproducibility. The physical parameters of aging were fixed at a temperature of 110 °C and an air flow rate of 166.7 ml/min. The blends were prepared by incubating C18:1-methyl ester pure and with 20 wt% acetic acid at room temperature. The weights for C18:1 was 3 g (pure and in the blend). The weight of acetic acid in the blend was 0.6 g. Samples were collected at time points of 0, 2, 4, 6, 8 and 10 h. In order to provide an overview over a longer period of time, aging was also taken into account for 10, 20, 30, 40, 50, 60, 70, 80, 90, and 100 h. Samples were either stored at – 20 °C or directly diluted [1:40 with 100 % ethanol with 0.5 % formic acid (v/v)]

and transferred to 1.5 ml glass screw-top vials (ND8) from Altmann Analytik GmbH & Co. KG, Germany, for LC-MS analysis.

4.3. Liquid chromatography

LC separation was performed on a Bruker Elute SP HPLC system equipped with three serially connected SEC columns. The specifications are listed in the supporting information. The column oven temperature was maintained at 40 °C. The mobile phase consisted of 100 % ethanol with 0.5 % formic acid (v/v) from Merck KGaA, Germany. A linear gradient was used over 60 min at a constant flow rate of 1.000 µL/min. The total runtime was 60 min. Injection volume was 10 µL.

4.4. Mass spectrometry

Mass spectrometric analysis was carried out using a Bruker Impact II ESI-QTOF-MS (Bruker Daltonics GmbH & Co. KG, Germany) coupled directly to the Bruker Elute SP HPLC system via an electrospray ionization (ESI) source operating in positive and negative ion mode. The following MS settings were applied based on method optimization and manufacturer recommendations (see supporting information).

Initial MS instrument calibration was performed prior to each analysis using Agilent TuningMix ESI-L low concentration tune mix (Agilent Technologies Deutschland GmbH, Germany) via direct infusion (at a flowrate of 3 µl/min) using a syringe pump LA-60 (Landgraf Laborsysteme HLL GmbH, Germany). Data were acquired using Compass Hystar software (ver. 6.3.1.8) and further processed using DataAnalysis (ver. 6.2.130.1.0) and MetaboScape 2025 (ver. 14.0.3.14016) for peak picking, feature annotation, and tentative identification of degradation or transformation products (Bruker Daltonics GmbH & Co. KG, Germany).

4.5. Data processing and compound identification

All spectra were automatically recalibrated (see supporting information), in addition to the initial instrument calibration prior to each analysis, post LC-MS data acquisition using feature extraction including MS/MS data for identification of acyl degradation products, oligomers, or other derivatives formed during acid-induced transformation. Tentative identification was performed based on accurate mass (< 2 mDa error), isotopic pattern matching, and fragment ion interpretation, if MS/MS data was available for respective precursors of interest.

4.6. Kinetical analysis

For kinetic analysis, concentrations were expressed in counts μL^{-1} using the injection volume (10 µL) as the reference volume. These values were used to quantify both the formation and decay of aging products over time. Because product formation followed exponential behavior, concentration data were logarithmically transformed to obtain linear relationships. The slope of the corresponding linear regression was defined as the apparent build-up rate constant. As the aging products represented reaction intermediates, they were treated as reactants after reaching their maximum concentration, and the subsequent decay phase was evaluated separately. The reaction order of the decay process was first determined, and the associated rate constants were then obtained by graphical analysis. Linear regressions used to determine both build-up and decay rate constants are provided in the supporting information.

CRediT authorship contribution statement

Julian Türck: Writing – original draft, Validation, Methodology, Data curation, Conceptualization. **Carsten Funke:** Writing – review & editing, Methodology, Investigation, Data curation. **Fabian Schmitt:** Writing – review & editing, Methodology, Data curation. **Jan Schneider:** Writing – review & editing, Validation. **Hans-Jürgen Danneel:** Writing – review & editing, Validation. **Ralf Türck:** Writing – review & editing, Resources, Project administration, Funding acquisition. **Wolfgang Ruck:** Writing – review & editing, Supervision. **Jürgen Krahl:** Writing – review & editing, Validation, Supervision, Project administration, Funding acquisition, Conceptualization.

Declaration of competing interest

The authors declare that they have no known competing financial interests or personal relationships that could have appeared to influence the work reported in this paper.

Appendix A. Supplementary data

Supplementary data to this article can be found online at https://doi.org/10.1016/j.fuel.2026.139339.

Data availability

Data will be made available on request.

References

[1] Tuerck J, et al. Solketal as a renewable fuel component in ternary blends with biodiesel and diesel fuel or HVO and the impact on physical and chemical properties. Fuel 2022;310:122463.
[2] Ramos MJ, et al. Influence of fatty acid composition of raw materials on biodiesel properties. Bioresour Technol 2009;100(1):261–8.
[3] Miraboutalebi SM, et al. Fatty acid methyl ester (FAME) composition used for estimation of biodiesel cetane number employing random forest and artificial neural networks: a new approach. Fuel 2016;166:143–51.
[4] Kleinová A, et al. Cold flow properties of fatty esters. Process Saf Environ Prot 2007;85(5):390–5.
[5] Yuan M-H, et al. Dependence of cold filter plugging point on saturated fatty acid profile of biodiesel blends derived from different feedstocks. Fuel 2017;195:59–68.
[6] Wang, C.-c., et al. (2021). "Comparison of reactive sites of different fatty acid molecules by quantum chemistry calculation.".
[7] Blanksby SJ, Ellison GB. Bond dissociation energies of organic molecules. Acc Chem Res 2003;36(4):255–63.
[8] Longanesi L, et al. Oxidative stability of biodiesel: recent insights. Biofuels Bioprod Biorefin 2022;16(1):265–89.
[9] Frankel EN. Lipid oxidation: mechanisms, products and biological significance. J Am Oil Chem Soc 1984;61(12):1908–17.
[10] Zuleta EC, et al. The oxidative stability of biodiesel and its impact on the deterioration of metallic and polymeric materials: a review. J Braz Chem Soc 2012;23:2159–75.
[11] Kpan JD, Krahl J. The impact of adsorbents on the oxidative stability of biodiesel and its influence on the deterioration of engine oil. Fuel 2019;256:115984.
[12] Strömberg N, et al. Biodiesel degradation rate after refueling. Fuel 2013;105:301–5.
[13] Türck J, et al. Oxidation Kinetics of Neat Methyl Oleate and as a Blend with Solketal. Energies 2023;16(7):3253.
[14] Fang, H. L. and R. L. McCormick (2006). Spectroscopic study of biodiesel degradation pathways, SAE technical paper.
[15] Singh P, et al. Impact of dual biofuel approach on engine oil dilution in CI engines. Fuel 2017;207:680–9.
[16] Meng Y, et al. Reactivity and structure: epoxidation of cottonseed oil and the corresponding fatty acid methyl ester. Biomass Convers Biorefin 2025;15(3):3333–44.
[17] Flitsch S, et al. Quantitation of aging products formed in biodiesel during the rancimat accelerated oxidation test. Energy Fuel 2014;28(9):5849–56.
[18] Pullen J, Saeed K. An overview of biodiesel oxidation stability. Renew Sustain Energy Rev 2012;16(8):5924–50.
[19] Türck J, et al. Extension of biodiesel aging mechanism–the role and influence of Methyl Oleate and the contribution of Alcohols through the use of Solketal. ChemSusChem 2023;16(17):e202300263.
[20] Yaakob Z, et al. A review on the oxidation stability of biodiesel. Renew Sustain Energy Rev 2014;35:136–53.
[21] Feng Y, et al. Identification of double bond position isomers in unsaturated lipids by m-CPBA epoxidation and mass spectrometry fragmentation. Anal Chem 2019;91(3):1791–5.
[22] Koritzke AL, et al. Fragmentation mechanisms from electron-impact of complex cyclic ethers formed in combustion. Int J Mass Spectrom 2020;454:116342.
[23] Sparkman OD, et al. Gas chromatography and mass spectrometry: a practical guide. Academic press; 2011.